

Epigenetics Programme, the Babraham Institute, Cambridge, United Kingdom, Mass Spectrometry, the Babraham Institute, Cambridge, United Kingdom, Centre for Trophoblast Research, University of Cambridge, Cambridge, United Kingdom

**Background:** DNA methylation is reprogrammed during early embryogenesis by active and passive mechanisms in advance of the first differentiation event producing the embryonic and extraembryonic lineage cells which contribute to the future embryo proper and to the placenta respectively. Embryonic lineage cells re-acquire a highly methylated genome dependent on the DNA methyltransferases (DNMTs) Dnmt3a and Dnmt3b that are required for *de novo* methylation. By contrast, extraembryonic lineage cells remain globally hypomethylated but the mechanisms that underlie this hypomethylation remain unknown.

**Methodology/Principal Findings:** We have employed an inducible system that supports up to 100% of the genome to be demethylated in a cell type-specific manner.

Importantly, in trophoblast giant cells Dnmt1 fails to be attracted to replication forks, leading to a loss of DNA methylation while implicating a passive demethylation mechanism. Interestingly, Dnmt1 targeting to replication forks by the exogenous Np95/Uhrf1, a Dnmt1 chaperone required for Dnmt1-targeting to replication forks, failed to increase methylation levels. Over-expression of *de novo* DNMTs also failed to increase methylation levels in these sequences.

**Conclusions/Significance:** We propose that induced trophoblast cells may have a resistance to DNA methylation, thus reinforcing the genome-wide epigenetic distinction between embryonic and extraembryonic lineages in the mouse. This resistance may be based on transcriptional differences in chromatin structure.

Oda M, Oxley D, Dean W, Reik W (2013) Regulation of Lineage Specific DNA Hypomethylation in Mouse Embryos. *PLOS ONE* 8(6): e68846. doi:10.1371/journal.pone.0068846

Jason Glenn Knott, Michigan State University, United States of America

October 4, 2012;

June 5, 2013;

June 25, 2013

© 2013 Oda et al. This is an open-access article distributed under the terms of the Creative Commons Attribution License, which permits unrestricted use, distribution, and reproduction in any medium, provided the original author and source are credited.

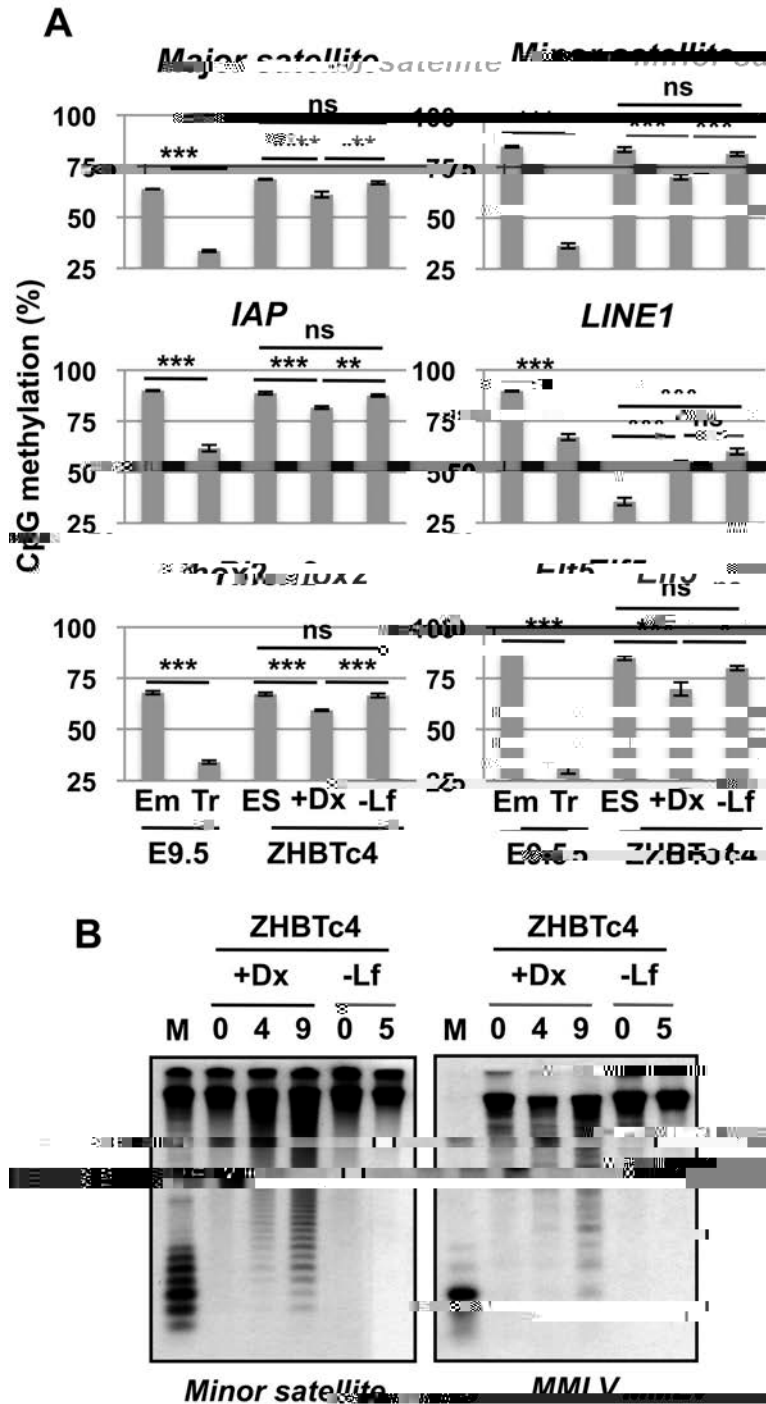
BBSRC; grant BB/H088071/1 ([www.bbsrc.ac.uk](http://www.bbsrc.ac.uk)), MRC; grant G0700760 ([www.mrc.ac.uk](http://www.mrc.ac.uk)), EU EpiGenome Consortium (EpiGenome BLUEPRINT; [www.blueprint-epigenome.eu](http://www.blueprint-epigenome.eu)). The funders had no role in study design, data collection and analysis, decision to publish, or preparation of the manuscript.

The authors note that Wendy Dean, one of the authors, is a PLOS ONE Editorial Board member. All authors have read and approved the final manuscript. We adhere to all the PLOS ONE policies on sharing and materials.

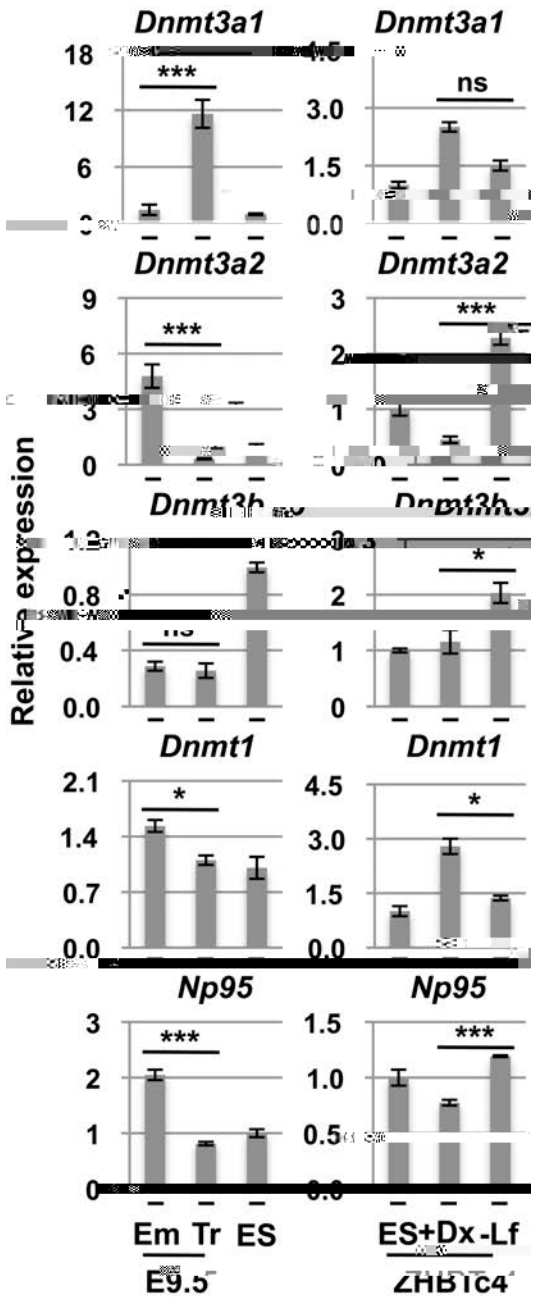
\* E-mail: [jknott@msu.edu](mailto:jknott@msu.edu) (Jason Glenn Knott), [wendy.dean@plosone.org](mailto:wendy.dean@plosone.org) (Wendy Dean), [reik@cam.ac.uk](mailto:reik@cam.ac.uk) (Walter Reik)

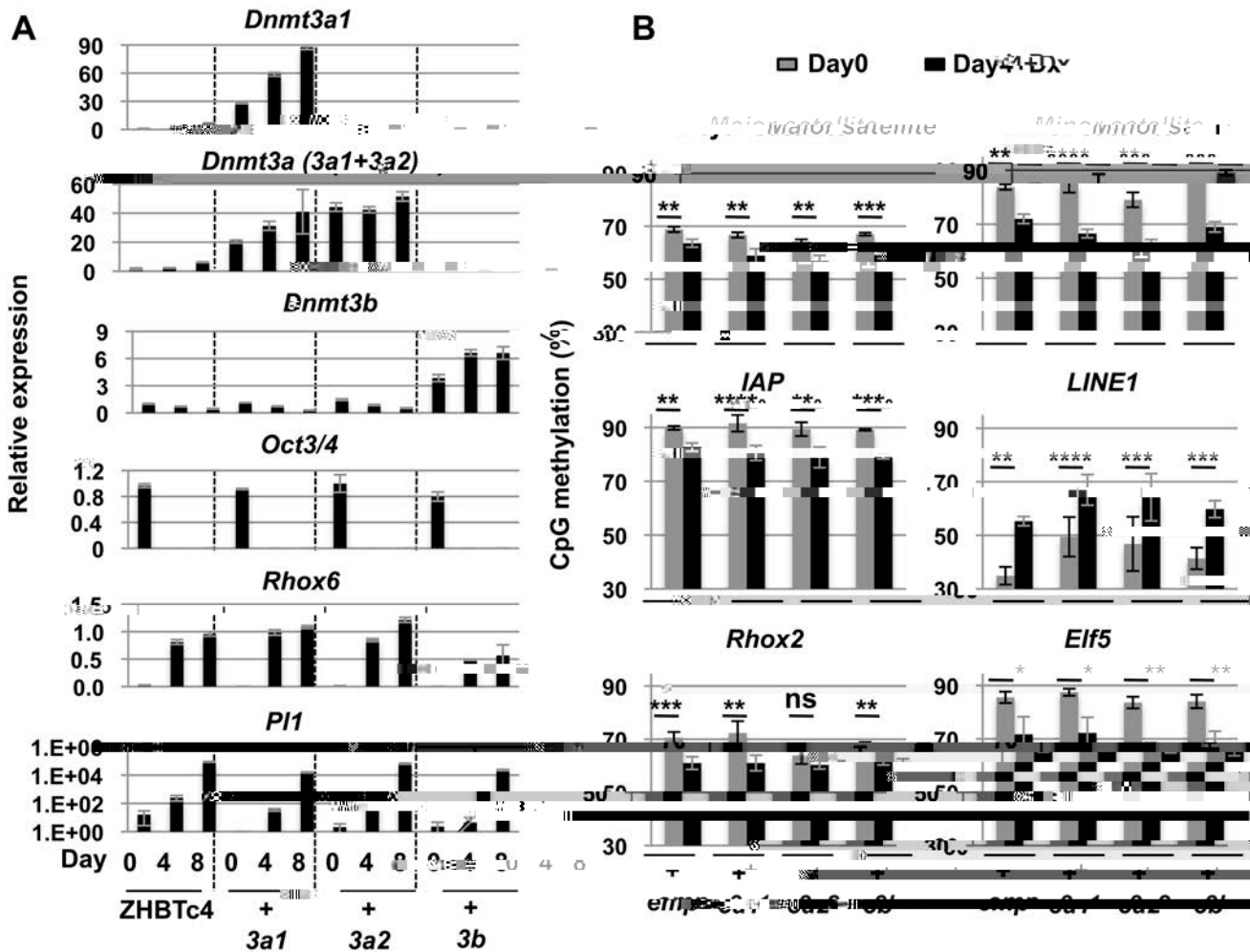
During the reprogramming process of early development, the first differentiation event prior to implantation gives rise to the two cell lineages, the embryonic and extraembryonic trophoblast lineage which contributes to the embryo proper and the extraembryonic tissue respectively including the placenta. It is now largely accepted that interactions between signaling events, transcription factor networks, and epigenetic regulation are involved in establishing these first two cell lineages. For example, the transcriptional regulator *Elf5* which is important for trophoblast cell fate is epigenetically silenced by DNA methylation in embryonic trophoblasts.

embryo proper and hypomethylated in extraembryonic trophoblast cells at E9.5 (Figure 1A). Methylation of retrotransposons of the IAP and LINE 1 families also shows this pattern albeit to a lesser deg



(A) The percentage of CpG methylation analyzed by Sequenom which averages the methylation of CpG methylation across each region. Embryo proper (Em) and trophoblast cells (Tr) are from E9.5 conceptus. ZHBTc4 ES-derived trophoblast cells (+Dx) and embryonic cells (-Lf) are differentiated by addition of doxycycline or removal of LIF respectively. Genomic DNA was collected at day 4 after differentiation. Values are means  $\pm$  standard deviation (SD) of biological replicates (n=3-4). \*\*\*:  $p < 0.001$ , \*\*:  $p < 0.01$ , \*:  $p < 0.05$ , ns: not significant; t-test and ANOVA followed by



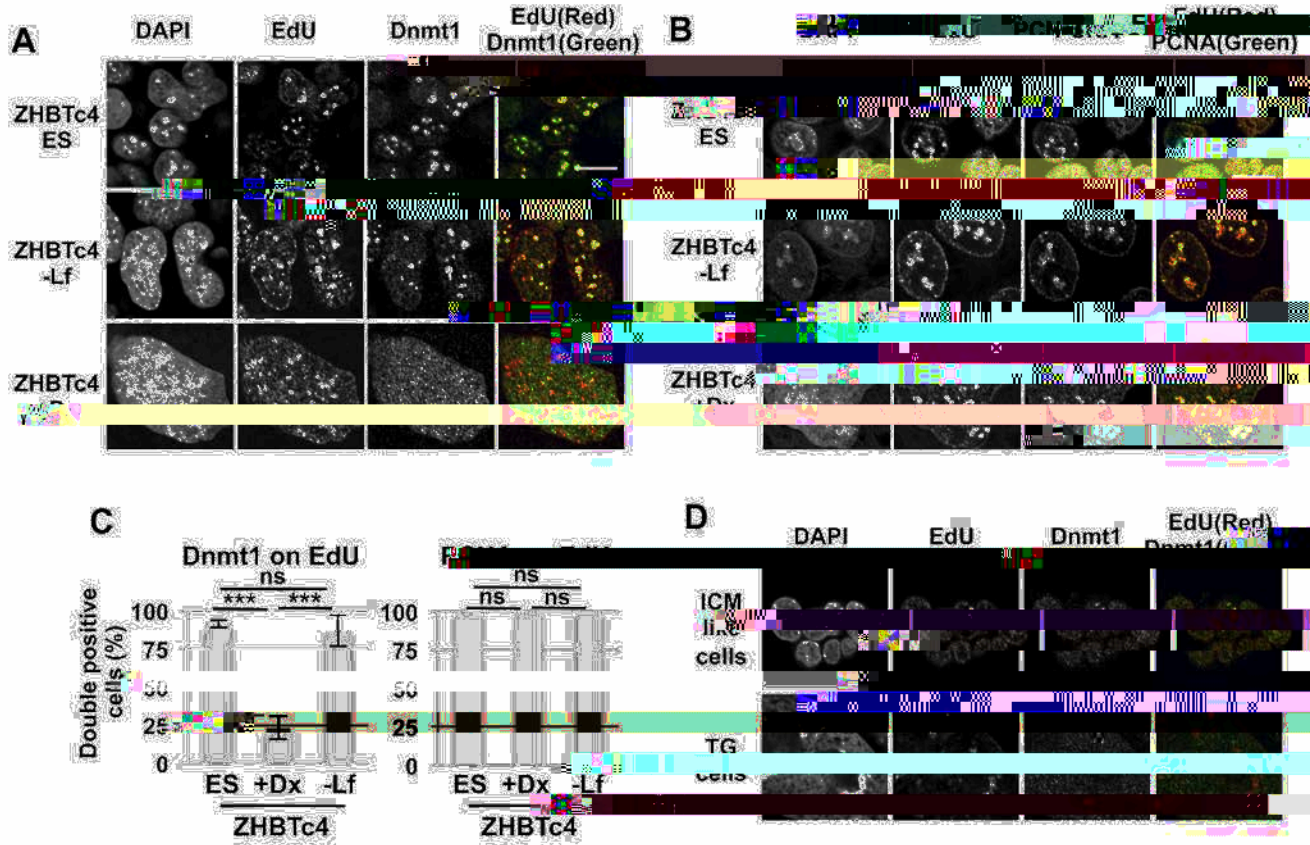


(A) mRNA expression of *Dnmt3* genes, *Oct3/4*, *Rhox6* and *Plate 1* during ZHBTc4 trophoblast differentiation with/without overexpression of exogenous *Dnmt3a1* (3a1), *Dnmt3a2* (3a2) or *Dnmt3b* (3b). A representative clone from each group of *Dnmt3*-expressing stable clone is shown in the figure. Values are means  $\pm$  SD of technical replicates ( $n=3$ ). Other clones in each group showed similar levels of expression of *Dnmt3* genes and marker genes. (B) DNA methylation analysis by Sequenom in ZHBTc4 ES cells and trophoblast cells with/without overexpression of exogenous *Dnmt3a1* (3a1), *Dnmt3a2* (3a2) or *Dnmt3b* (3b). emp: empty vector. A gray column indicates ES cell data (Day 0). A black column indicates data from trophoblast cells induced by the addition of doxycycline (Day4+Dx). Values are means  $\pm$  SD of biological replicates ( $n=3-5$ ) except for the value of major satellite for empty vector day 4 whose value is shown as the mean of biological duplicate. So, there is no stats for the value of major satellite at day 4. \*\*\*\*:  $p<0.0001$ , \*\*\*:  $p<0.001$ , \*\*:  $p<0.01$ , \*:  $p<0.05$ , ns: not significant; paired t-tests.

doi: 10.1371/journal.pone.0068846.g003

strand at DNA replication foci during S-phase [30,31]. The transcription level of Np95 was lower in E9.5 trophoblast cells or ZHBTc4+Dox cells than embryo proper or ZHBTc4-Lif cells (Figure 2A and B). Furthermore, its expression decreased during the differentiation from TS cells to TG cells (Figure S3C). There is, however, still the possibility that the difference in transcriptional level can be caused by the difference of cell cycle status because the expression of Np95 is tightly regulated in a cell cycle dependent manner [32].

To focus on the Np95 protein itself in S-phase cells, we stained Np95 and visualized S-phase cells by EdU. As reported previously, Np95 localized to replication foci together with Dnmt1 in ES cells and TS cells (Figure S3D). However, we found that Np95 was not localized to replication foci of TG cells derived from both ZHBTc4 cells and TS cells (Figure 5A and Figure S3D). It appeared that Np95 was completely absent from nuclei of TG cells as seen in *Np95*<sup>-/-</sup> knockout (KO) ES cells. Next we hypothesized that repression of Np95 might



(A,B) Immunostaining analysis of ZHBTc4 ES cells and ZHBTc4-derived embryonic (-Lf) and trophoblast cells (+Dx) at day 4 after differentiation using antibodies against Dnmt1 (A) and PCNA (B). Replication sites were visualized by the incorporation of the nucleotide analogue EdU. DNA was visualized with DAPI. Merged images represent overlays of immunofluorescence signal of Dnmt1 or PCNA (green) and EdU (red). (C) The score of Dnmt1 or PCNA localization at replication site in ZHBTc4 ES cells and trophoblast cells at day 4 after doxycycline induction (+Dx). Nuclear size was analyzed by ImageJ and divided into three categories (size similar to nucleus of ES cells, twice the size, and larger). Values are means  $\pm$  SD of biological replicates (n=4-7 for Dnmt1, n=3-4 for PCNA). \*\*\*: p<0.001, ns: not significant; ANOVA and Bonferroni's multiple comparison test. (D) Immunostaining analysis of blastocyst outgrowths using antibodies against Dnmt1. DNA and replication sites were visualized with DAPI and EdU respectively. Scale bar, 10  $\mu$ m.

doi: 10.1371/journal.pone.0068846.g004

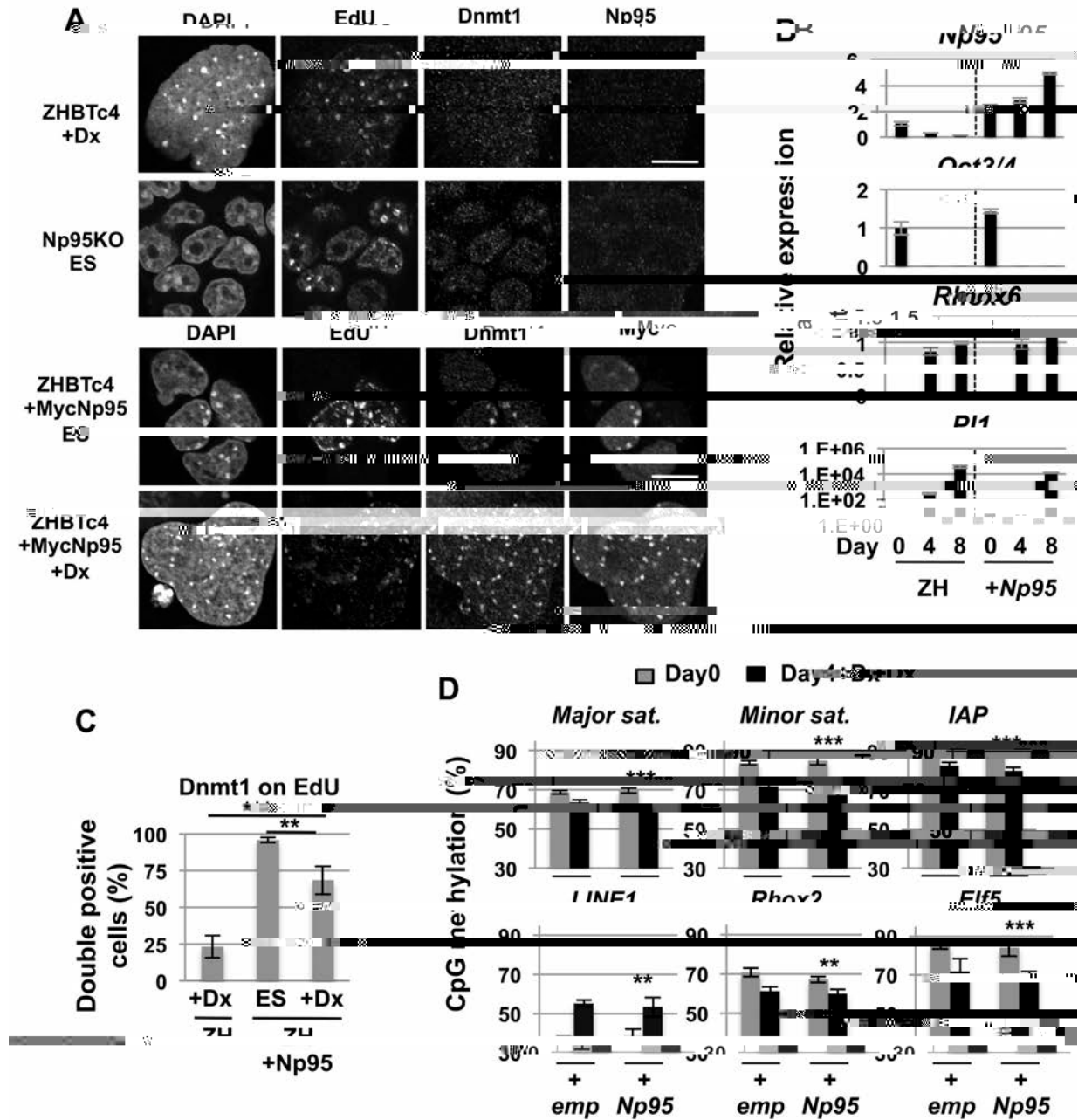
result in mis-localization of Dnmt1 and/or result in a reduction of DNA methylation during trophoblast differentiation.

On induced transdifferentiation, ZHBTc4+Dox cells have no detectable levels of Np95 (Figure 5A). To attempt to restore DNA methylation mediated by Dnmt1 recruitment, forced overexpression of a Myc-tagged Np95 (MycNp95) was engineered to be coupled to ZHBTc4 transdifferentiation (ZHBTc4+Dox+MycNp95).

It was confirmed that exogenous MycNp95 was targeted to replication foci and capable of restoring DNA methylation in *Np95* KO ES cells (Figure S4B, C) [30]. The *MycNp95* gene was more highly expressed than endogenous *Np95* gene and stably expressed even after ZHBTc4+Dox differentiation (Figure 5B). ZHBTc4+Dox+MycNp95 cells showed similar

expression levels of *Plate 1* and *Rhox6* and were morphologically similar to control ZHBTc4+Dox cells (Figure 5B and data not shown). Immunostaining confirmed the colocalization of MycNp95 and Dnmt1 to EdU labeled replication foci in middle-late S phase in ZHBTc4 ES+MycNp95 cells and in ZHBTc4+Dox+MycNp95 cells (Figure 5A and C). Thus overexpression of MycNp95 was able to improve Dnmt1 association to replication sites *in vitro*. Importantly temporal progression did not appear to be affected by the 5-fold increase in Np95 expression (Figure 5B). However, despite driving Dnmt1 to replication foci by overexpression of MycNp95, DNA methylation of target sequences was unaffected (Figure 5D). Thus, lower expression of Np95 may not account for global hypomethylation during trophoblast differentiation.

Thus, decline in DNA methylation in ZHBTc4+Dox differentiation is not simply a consequence of the absence of Dnmt1 at replication forks owing to insufficient expression of an



(A) Immunostaining analysis of ZHBTc4-derived trophoblast cells (+Dx), Np95-KO ES cells, ZHBTc4 ES cells overexpressing exogenous Np95 (+MycNp95 ES) and ZHBTc4-derived trophoblast cells overexpressing exogenous Np95 (+MycNp95+Dx) using antibodies against Dnmt1, Np95 or Myc. DNA and replication sites were visualized with DAPI and EdU respectively. Scale bar, 10  $\mu$ m. (B) mRNA expression of *Np95*, *Oct3/4*, *Rhox6* and *Plat1* genes during ZHBTc4 trophoblast differentiation with (+Np95) or without (ZH) overexpression of exogenous Np95. A representative clone for Np95-overexpressing ZHBTc4 cells is shown in the figure. Values are means  $\pm$  SD of technical replicates (n=3). Other independent clones also showed similar results for marker gene and Np95 expression. (C) Dnmt1 localization at replication site in Np95-overexpressing ZHBTc4-derived trophoblast cells at day 4 after differentiation. The control data in ZHBTc4-derived trophoblast cells (ZH+Dx) is identical to ZHBTc4+Dx of Figure 4C. Values are means  $\pm$  SD of biological replicates (n=3). \*\*\*,  $p < 0.001$ , \*\*,  $p < 0.01$ , ns: not significant; ANOVA and Bonferroni's multiple comparison test. (D) DNA methylation analysis by Sequenom in ZHBTc4 ES (Day0) and ZHBTc4-derived trophoblast cells (Day4+Dx) with (+Np95) or without (ZH) overexpression of exogenous Np95. The control data (+emp) is identical to the data of +emp in Figure 3B. Values are means  $\pm$  SD of biological replicates (n=3-5). \*\*\*,  $p < 0.001$ , \*\*,  $p < 0.01$ ; paired t-tests.

doi: 10.1371/journal.pone.0068846.g005



obligate chaperone, Np95. Rather loss of DNA methylation appears to be a consequence of some intrinsic setting of DNA methylation to ensure a hypomethylated landscape in the trophoctoderm lineage.

In this study, using an *in vitro* differentiation system of ES and TS cells which can recapitulate the developmental processes around implantation, we focused on the first two cell lineages in development, embryonic and extraembryonic trophoblast cells, as a model system to address cell-type specific regulation of DNA methylation. *In vivo*, demethylation begins in the zygote and by the blastocyst stage (by which the trophoctoderm has been established) global hypomethylation has been achieved [33], which is then largely maintained in the trophoblast lineage. This demethylation is achieved by a combination of active (including hydroxylation by the Tet family of enzymes) and passive processes (including cytoplasmic retention of Dnmt1). By contrast, there is dramatic *de novo* methylation in embryonic tissues starting at implantation which depends on Dnmt3a and Dnmt3b. Interestingly, DNA methylation deficient ES cells efficiently differentiate into extraembryonic cells [5].

Here

All experimental procedures were conducted under licenses by the Home Office (UK) in accordance with the Animals (Scientific Procedures) Act 1986. Extraembryonic trophoctoderm tissues and embryo proper from C57BL/6 were dissected under a microscope. Our quantitative RT-PCR analysis confirmed no contamination among extraembryonic tissue and embryo proper. Blastocyst outgrowths were obtained by culturing blastocysts from a cross of (C57BL/6 x CBA/Ca) F1 females mated to (C57BL/6 x CBA/Ca) F1 males in DMEM with 10% FBS for 3-5 days.

ES cells were maintained as described previously [14]. The cells were grown on gelatin-coated culture dishes without feeder cells in standard ES cell medium.

For trophoblast differentiation by Oct3/4 down regulation, 1 µg/ml doxycycline (Sigma) was added to the ES culture medium of ZHBTc4 ES cells. For embryonic differentiation, LIF was withdrawn from ES culture medium.

For replication labeling, cells were incubated for 10 min in medium containing 20 µM EdU (5-ethynyl-2'-deoxyuridine), a nucleotide analogue to thymidine, which is detected by click chemistry with the Click-iT kit (Invitrogen) and were harvested for immunostaining.

Plasmid vectors for the expression of Dnmt3a, Dnmt3a2, Dnmt3b or Np95 were generated by subcloning the corresponding cDNAs into the pCAG-IRESpuro expression vector that contains the CAG promoter (a synthetic promoter that includes the chicken- $\beta$ -actin promoter and the human cytomegalovirus immediate early enhancer) [13,30]. These constructs were individually electroporated into ZHBTc4 ES cells, which were subsequently selected in puromycin (Sigma) -containing medium for stable clones.

Total RNA was isolated using an Allprep DNA/RNA mini kit (Qiagen) according to the manufacturers' protocol. For RT-PCR, cDNA was synthesized from 0.5–1 µg of total RNA with random hexamers and Superscript III reverse transcriptase (Invitrogen). Quantitative PCR was performed with Brilliant II SYBR Green QPCR Master Mix (Agilent) using MX3005P (Stratagene) or CFX96 Real-Time system (Bio-Rad). *Hspcb* and *Atp5b* genes were used for normalization. Sequences of primers for PCR are available from the authors on request.

Cells cultured on coverslips were fixed with 4% paraformaldehyde (Sigma) for 15 min at room temperature or methanol (BDH) for 4 min at -20C, and permeabilised with PBS containing 0.5% Triton X-100 for 20 min at room temperature. Fixed materials were blocked in 0.05% Tween-20 in PBS containing 1% BSA for 30 min at room temperature and incubated for 45 min at room temperature with primary antibodies against Dnmt1 (H-300, Santa Cruz), PCNA (PC10, Santa Cruz), Np95 (Th10), or Myc epitope tag (Millipore). Detection was achieved using Alexa Fluor 488, 568, 594 or 647 labeled anti anti-mouse, anti-rat or anti-rabbit IgG antibody

(Invitrogen) as secondary antibodies. DNA was stained with 1 µg/ml DAPI (Invitrogen) and all samples were mounted in SlowFade Gold antifade reagent (Invitrogen). Images were acquired using a laser scanning confocal microscope (FV1000, Olympus). Nuclear sizes were measured using ImageJ software.

Genomic DNA was isolated using an Allprep DNA/RNA mini kit (Qiagen) according to the manufacture's protocol. For methylation analysis of CpG units at specific regions using MassArray® system (Sequenom) analysis, Sodium bisulfite treatment of genomic DNA was performed using an Epiect Bisulfite Kit (Qiagen). Converted DNA was amplified by HotStarTaq DNA polymerase (Qiagen). Sequences of PCR primers and PCR conditions are available from the authors on request. The subfamily of LINE 1 analyzed in the Sequenom analysis is LINE 1 A.

For DNA methylation analysis by southern blotting, genomic DNA was digested with the CpG methylation-sensitive or – insensitive restriction enzymes HpaII (Fermentus) or MspI (Fermentus), and subjected to southern blotting. The blot was hybridized with probes for minor satellite repeats or C-type endogenous retroviruses (MMLV).

For the analysis of methylation within total cytosine by mass-spectrometry, genomic DNA was digested with DNA degradase plus (ZYMO RESEARCH) and subjected to mass spectrometry (liquid chromatography electrospray ionization tandem mass spectrometry).

(A) Total amount of methylcytosine analyzed by mass-spectrometry in ES, TS, and TS-derived trophoblast giant (TG) cells. TG cells are day 5 after differentiation. Values are means  $\pm$  SD of technical replicates (n=3). (B) DNA methylation analysis by Sequenom in ES, TS and TS-derived TG cells. TG cells are day 5 after differentiation. Values are means  $\pm$  SD of technical replicates (n=3). (C) mRNA expression of *Np95*, *Dnmt1*, *Oct3/4*, *Zfp42*, *Cdx2*, *Plat1*, *beta-actin*, and *Gapdh* genes in wild-type ES, *Np95*<sup>-/-</sup> KO ES, TS and TS-derived TG cells. PCR cycles are shown on the right. (D) Immunostaining analysis of ES, TS, and TS-derived TG cells using antibodies against Dnmt1 and Np95. Replication sites and DNA were visualized by the incorporation of nucleotide analogue EdU and DAPI respectively. Merged images represent overlays of immunofluorescence signal of Np95 (green) and Dnmt1 (red). Scale bar, 10  $\mu$ m. (TIF)

cells using antibodies against Dnmt1 and Myc which detects exogenous Np95. DNA and replication sites were visualized with DAPI and EdU.

elyz

(A) DNA methylation profile of the genomic region around *Rhox6/9* (target of Dnmt3a and Dnmt3b), *Ube2a* (non-target of Dnmt3a and Dnmt3b) and the region without HpaII site (No HpaII) obtained by HpaII-digestion PCR. Genomic DNA was digested with (+) or without (-) HpaII which is sensitive to CG methylation and was subjected to PCR. Loss of *Rhox6/9* methylation was restored by the exogenous Dnmt3a1, Dnmt3a2 or Dnmt3b. Independent stable clones are shown as #1, #2 or #3. (B) The percentage of CpG methylation analyzed by Sequenom. Loss of methylation in *Np95* KO ES cells was restored by the exogenous Np95 (MycNp95). Values are means  $\pm$  SD of technical replicates (n=3) except for the value of major satellite for *Np95*KO and +MycNp95 whose values are shown as the mean  $\pm$  error bar of biological duplicate. (C) Immunostaining analysis of rescued (+MycNp95) *Np95* KO ES

linked homeobox gene cluster in a lineage-specific manner. *Genes Dev* 20: 3382-3394. doi:10.1101/gad.1470906. PubMed: 17182866.

14. Niwa H, Miyazaki J, Smith AG (2000) Quantitative expression of Oct-3/4 defines differentiation, dedifferentiation or self-renewal of ES cells. *Nat Genet* 24: 372-376. doi:10.1038/74199. PubMed: 10742100.
15. Lee HJ, Hinshelwood RA, Bouras T, Gallego-Ortega D, Valdés-Mora F et al. (2011) Lineage specific methylation of the Elf5 promoter in mammary epithelial cells. *Stem Cells* 29: 1611-1619. doi:10.1002/stem.706. PubMed: 21823211.
16. Mouse Genome Sequencing Consortium, Waterston RH, Lindblad-Toh K, Birney E, Rogers J (2002) Initial sequencing and comparative analysis of the mouse genome. *Nature* 420: 520-562. doi:10.1038/nature01262. PubMed: 12466850
17. Ficz G, Branco MR, Seisenberger S, Santos F, Krueger F et al. (2011) Dynamic regulation of 5-hydroxymethylcytosine in mouse ES cells and during

PubMed: 218268 7 M Ficy